Photochemical Dealkylation of the Bridging Phosphite-Type Ligand $(Pr^iO)_2PN(Et)P(OPr^i)_2$ in the Electronically Unsaturated Diruthenium Complex $[Ru_2(\mu_{sb}\text{-}CO)_2(CO)_2\{\mu\text{-}(Pr^iO)_2PN(Et)P(OPr^i)_2\}_2]$

Robert M. Granger II,[†,∥] Phillip E. Fanwick,*[,‡] Raymond J. Haines,*[,§] and Clifford P. Kubiak*[,†]

Departments of Chemistry, Purdue University, 1393 Brown Laboratory, West Lafayette, Indiana 47907, and University of Natal, P.O. Box 375, Pietermaritzburg 3200, South Africa

Received January 28, 1993

Earlier studies by Haines and co-workers[1-4] revealed that coordinated tertiary phosphite ligands can, under appropriate reaction conditions, be dealkylated to afford phosphonate products via an Arbuzov (Michaelis-Arbuzov)-type mechanism. In particular, it was established that the reaction of $[Mo_2(\eta^5\text{-}C_5H_5)_2(CO)_6]$ and $[Fe(\eta^5\text{-}C_5H_5)(CO)_2Cl]$ with trimethyl phosphite affords $[Mo(\eta^5\text{-}C_5H_5)(CO)_2\{P(OMe)_3\}P(O)(OMe)_2]$ and $[Mo(\eta^5\text{-}C_5H_5)(CO)_3CH_3]$ and $[Fe(\eta^5\text{-}C_5H_5)(CO)_2P(O)(OMe)_2]$, respectively, with the final steps in the reactions involving nucleophilic attack of $[Mo(\eta^5\text{-}C_5H_5)(CO)_3]^-$ and Cl^- on the cationic (phosphonium ion) intermediates $[Mo(\eta^5\text{-}C_5H_5)(CO)_2\{P(OMe)_3\}_2]^+$ and $[Fe(\eta^5\text{-}C_5H_5)(CO)_2P(OMe)_3]^+$, respectively.[1-4] This transformation of tertiary alkyl phosphites on metal centers has since attracted substantial attention,[5,6] and moreover, it is now recognized that metal-containing Arbuzov-type products can also be formed in the reactions of metal complexes with tertiary alkyl phosphites via radical pathways,[5] although the number of examples of the latter type of reaction is limited.[7-9] We note that the susceptibility of uncoordinated alkyl phosphites to radical attack is well established.[10-13]

We recently reported that the electron-rich tetraisopropoxy-diphosphazane-bridged derivative of diruthenium nonacarbonyl, $[Ru_2(\mu\text{-}CO)(CO)_4\{\mu\text{-}(Pr^iO)_2PN(Et)P(OPr^i)_2\}_2]$ (**1**), can be decarbonylated under thermal conditions to afford the electronically unsaturated species $[Ru_2(\mu_{sb}\text{-}CO)_2(CO)_2(\mu\text{-}(Pr^iO)_2PN(Et)P(OPr^i)_2\}_2]$ (sb = semibridging) (**2**).[14] This intensely purple compound is highly susceptible to nucleophilic as well as electrophilic attack. Indeed, the recently reported $\mu\text{-}CO_2$ diruthenium complex $[Ru_2\{\mu\text{-}\eta^2\text{-}OC(O)\}(CO)_4\{\mu\text{-}(Pr^iO)_2PN(Et)P(OPr^i)_2\}_2]$ (**3**) is conceptually related to **2** by simple addition of carbon dioxide across the two ruthenium atoms, although its synthesis in fact involves a less direct procedure.[15] Therefore, with the object of ascertaining whether complex **2** would add CO_2 directly by a photochemical pathway, its photochemistry in the presence of CO_2 was investigated. Instead of a photochemical reaction of **2** with CO_2, an unprecedented photochemical Arbuzov-type rearrangement of one of the diphosphazane ligands of **2** was observed.

Table I. Crystallographic Data for Complex **4**

$Ru_2P_4O_{13}N_2C_{30}H_{57}$	fw 979.83
a = 9.700(1) Å	space group $P2_1/c$ (No. 14)
b = 17.916(1) Å	T = 20 °C
c = 26.621(2) Å	λ = 1.541 84 Å
β = 99.255(8)°	ρ_{calcd} = 1.425 g cm^{-3}
V = 4565(1) Å^3	μ = 72.98 cm^{-1}
Z = 4	transm coeff = 0.44–1.00
$R(F_o)$ = 0.048[a]	$R_w(F_o^2)$ = 0.055[a]

[a] $R(F_o) = \sum||F_o| - |F_c||/\sum|F_o|$; $R_w(F_o^2) = [\sum w(F_o - F_c)^2/\sum wF_o^2]^{1/2}$.

Experimental Section

General Procedures. All manipulations were carried out under nitrogen using standard Schlenk line and drybox techniques. Solvents were degassed and purified by distillation under nitrogen from the appropriate drying agents. The complexes $[Ru_2(\mu\text{-}CO)(CO)_4\{\mu\text{-}(Pr^iO)_2PN(Et)P(OPr^i)_2\}_2]$ (**1**), $[Ru_2(\mu_{sb}\text{-}CO)_2(CO)_2\{\mu\text{-}(Pr^iO)_2PN(Et)P(OPr^i)_2\}_2]$ (**2**), and $[Ru_2(\mu_{sb}\text{-}CO)_2(CO)_2\{\mu\text{-}(MeO)_2PN(Et)P(OMe)_2\}_2]$ (**5**) were prepared by published literature methods.[14,16] ^1H NMR spectra were recorded on a Gemini 200 spectrometer, with chemical shifts reported in ppm referenced to external $SiMe_4$. $^{31}P\{^1H\}$ NMR spectra were recorded on a Varian XL-200 spectrometer at 80.96 MHz, with chemical shifts reported in ppm referenced to external H_3PO_4. Infrared spectra were recorded on a Perkin-Elmer 1710 FTIR spectrophotometer. UV–vis data were collected on an IBM 9420 UV–visible spectrophotometer. All GC data were collected on a CARLE Series S-158 gas chromatograph.

Synthesis of $[Ru_2H(CO)_5\{\mu\text{-}(Pr^iO)_2PN(Et)P(OPr^i)_2\}\{\mu\text{-}(Pr^iO)P(O)N(Et)P(OPr^i)_2\}]$ (4). Photolysis of all samples was conducted with an Oriel 1000-W Hg/Xe lamp using quartz cells attached by a graded quartz seal to a high-vacuum stopcock for convenient freeze–pump–thaw (FPT) sample preparation. Typically, 0.05 g of **2** and 5 mL of benzene were placed into an FPT cell and taken through three freeze–pump–thaw cycles on a high-vacuum line. Photolysis of samples so prepared with the unfiltered output of the UV lamp was essentially complete after 30 min. Removal of solvent resulted in a dark orange viscous oil. $^{31}P\{^1H\}$ NMR (C_6H_6): δ 153.0 (m, ABC), 74.7 ppm (m, X). ^1H NMR (C_6H_6): δ −7.12 ppm (q, Ru–*H*). IR (cm^{-1}, THF): ν(CO) 2057 w, 2019 s, 1985 s, 1963 sh, 1886 w.

X-ray Structure Determination of $[Ru_2H(CO)_5\{\mu\text{-}(Pr^iO)_2PN(Et)P(OPr^i)_2\}\{\mu\text{-}(Pr^iO)P(O)N(Et)P(OPr^i)_2\}]$ (4). The viscous oil isolated subsequent to photolysis crystallized after allowing the sample to stand for several days. A colorless needle of $C_{30}H_{57}Ru_2N_2O_{13}P_4$ having approximate dimensions of 0.31 × 0.20 × 0.17 mm was mounted in a glass capillary in a random orientation. Data were collected with Cu Kα radiation (λ = 1.541 84 Å) from a rotating anode source on an Enraf-Nonius CAD4 computer-controlled κ axis diffractometer equipped with a graphite crystal incident beam monochromator. The structure was solved using the structure solution program SHELX-86. The crystallographic data are summarized in Table I, the final atomic coordinates are given in Table II, an ORTEP drawing of **4** is presented in Figure 1, and selected bond distances and angles for **4** are listed in Tables III and IV, respectively.

Results and Discussion

The intense purple color of the unsaturated complex $[Ru_2(\mu_{sb}\text{-}CO)_2(CO)_2(\mu\text{-}(Pr^iO)_2PN(Et)P(OPr^i)_2\}_2]$ (**2**) results from a broad band in its UV–vis spectrum at 550 nm (ϵ = 20 000 M^{-1} cm^{-1}). The other dominant feature of the UV–vis spectrum of **2** is

† Purdue University.
‡ Author to whom crystallographic inquiries should be addressed at Purdue University.
§ University of Natal; on sabbatical leave at Purdue University from Dec 1991 to July 1992.
∥ Present address: Department of Chemistry, Virginia Military Institute, Lexington, VA 24450.

(1) Haines, R. J.; Marais, I. L.; Nolte, C. R. *Chem. Commun.* **1970**, 547.
(2) Haines, R. J.; Nolte, C. R. *J. Organomet. Chem.* **1970**, *24*, 725.
(3) Haines, R. J.; du Preez, A. L.; Marais, I. L. *J. Organomet. Chem.* **1970**, *24*, C26.
(4) Haines, R. J.; du Preez, A. L.; Marais, I. L. *J. Organomet. Chem.* **1971**, *28*, 405.
(5) Brill, T. B.; Landon, S. J. *Chem. Rev.* **1984**, *84*, 577.
(6) Alex, R. F.; Pomeroy, R. K. *Organometallics* **1982**, *1*, 453.
(7) Goh, L. Y.; D'Aniello, M. J.; Dlater, S.; Muetterties, E. L.; Tavanaiepour, I.; Chang, M. I.; Fredrich, M. F.; Day, V. W. *Inorg. Chem.* **1979**, *18*, 192.
(8) Howell, J. A. S.; Rowan, A. J. *J. Chem. Soc., Dalton Trans.* **1980**, 1894.
(9) Howell, J. A. S.; Rowan, A. J.; Snell, M. S. *J. Chem. Soc., Dalton Trans.* **1981**, 325.
(10) Walling, C.; Rabinowitz, R. *J. Am. Chem. Soc.* **1959**, *81*, 1243.
(11) Kochi, J. K.; Krusic, P. J. *J. Am. Chem. Soc.* **1969**, *91*, 3944.
(12) Davies, A. G.; Griller, D.; Roberts, B. P. *Angew. Chem., Int. Ed. Engl.* **1971**, *10*, 738.
(13) Bentrude, W. G.; Alley, W. D.; Johnson, N. A.; Murakami, M.; Nishikida, K.; Tan, H. W. *J. Am. Chem. Soc.* **1977**, *99*, 4383.
(14) Field, J. S.; Haines, R. J.; Sundermeyer, J.; Woollam, S. F. *J. Chem. Soc., Chem. Commun.* **1991**, 1382. Field, J. S.; Haines, R. J.; Stewart, M. W.; Sundermeyer, J.; Woollam, S. F. *J. Chem. Soc., Dalton Trans.*, in press.
(15) Field, J. S.; Haines, R. J.; Sundermeyer, J.; Woollam, S. F. *J. Chem. Soc., Chem. Commun.* **1990**, 985. Field, J. S.; Haines, R. J.; Sundermeyer, J.; Woollam, S. F. Submitted for publication.
(16) de Leeuw, G.; Field, J. S.; Haines, R. J.; McCulloch, B.; Meintjies, E.; Monberg, C.; Olivier, G. M.; Ramdial, P.; Sampson, C. N.; Sigwarth, B.; Steen, N. D.; Moodley, K. G. *J. Organomet. Chem.* **1984**, *275*, 99.

0020-1669/93/1332-3570$04.00/0

Table II. Positional Parameters and Their Estimated Standard Deviations for the Non-Hydrogen Atoms of Complex **4**

atom	x	y	z	B,[a] (Å^2)
Ru(1)	0.2476(1)	0.14668(5)	0.08306(3)	4.30(2)
Ru(2)	0.1645(1)	0.25130(5)	0.15543(3)	4.88(2)
P(11)	0.2219(3)	0.2362(2)	0.0173(1)	5.12(8)
P(12)	0.2695(3)	0.0554(2)	0.1459(1)	4.74(7)
P(21)	0.0987(3)	0.3332(2)	0.0889(1)	4.82(8)
P(22)	0.2648(4)	0.1728(2)	0.2197(1)	5.57(8)
O(11)	0.334(1)	0.0381(5)	0.0064(3)	9.6(3)
O(12)	0.5355(9)	0.2111(5)	0.1229(3)	8.1(3)
O(13)	-0.0655(9)	0.1271(5)	0.0472(4)	8.3(3)
O(21)	0.136(1)	0.3746(5)	0.2296(3)	10.2(3)
O(22)	-0.1228(9)	0.1788(6)	0.1520(4)	9.9(3)
O(111)	0.3687(8)	0.2798(4)	0.0152(3)	5.9(2)
O(112)	0.1636(9)	0.2090(4)	-0.0343(3)	6.1(2)
O(121)	0.146(1)	-0.0043(5)	0.1443(3)	7.7(3)
O(122)	0.391(1)	-0.0037(5)	0.1489(3)	8.9(3)
O(211)	-0.0639(7)	0.3552(4)	0.0765(3)	5.1(2)
O(212)	0.1606(8)	0.4168(4)	0.0985(3)	5.9(2)
O(221)	0.206(1)	0.1680(5)	0.2694(3)	10.9(3)
O(222)	0.426(1)	0.1869(5)	0.2445(4)	10.3(3)
N(1B)	0.1203(9)	0.3097(5)	0.0310(3)	4.7(2)
N(2B)	0.276(1)	0.0822(5)	0.2058(3)	5.4(2)
C(11)	0.303(1)	0.0785(7)	0.0351(4)	6.2(3)
C(12)	0.430(1)	0.1885(7)	0.1102(4)	6.0(3)
C(13)	0.052(1)	0.1335(7)	0.0632(4)	6.0(3)
C(21)	0.145(1)	0.3265(8)	0.2013(4)	6.8(4)
C(22)	-0.018(1)	0.2039(8)	0.1518(5)	6.4(4)
C(1B1)	0.069(1)	0.3608(7)	-0.0124(4)	5.9(3)
C(1B2)	-0.066(2)	0.3363(8)	-0.0420(5)	8.1(4)
C(2B1)	0.317(2)	0.0283(7)	0.2485(5)	9.2(5)
C(2B2)	0.209(3)	-0.022(1)	0.2581(7)	17.3(8)
C(1111)	0.490(2)	0.3406(9)	-0.0432(6)	11.0(5)
C(1112)	0.446(1)	0.2654(7)	-0.0261(5)	7.8(4)
C(1113)	0.571(2)	0.2194(9)	-0.0067(6)	10.6(5)
C(1211)	0.160(2)	-0.1252(9)	0.1056(9)	13.7(7)
C(1212)	0.094(1)	-0.0515(7)	0.1023(5)	6.8(4)
C(1213)	-0.054(2)	-0.057(1)	0.1029(9)	15.1(7)
C(1221)	0.561(2)	-0.068(1)	0.1130(8)	14.1(7)
C(1222)	0.526(1)	0.0050(8)	0.1341(5)	8.1(4)
C(1223)	0.627(2)	0.023(1)	0.1791(9)	15.5(8)
C(2111)	-0.158(2)	0.4755(8)	0.0888(7)	11.2(5)
C(2112)	-0.133(1)	0.3994(7)	0.1106(5)	6.2(3)
C(2113)	-0.268(1)	0.3616(9)	0.1147(6)	9.4(5)
C(2121)	0.346(2)	0.4659(8)	0.0633(7)	9.8(5)
C(2122)	0.308(1)	0.4339(7)	0.1094(5)	7.7(4)
C(2123)	0.328(2)	0.490(1)	0.1523(6)	15.5(6)
C(2211)	0.127(4)	0.217(2)	0.3390(8)	30(2)
C(2212)	0.098(2)	0.199(1)	0.2871(7)	14.3(6)
C(2213)	-0.009(3)	0.152(3)	0.288(1)	33(2)
C(2221)	0.551(3)	0.222(2)	0.318(1)	28(1)
C(2222)	0.488(2)	0.247(1)	0.2643(7)	14.5(6)
C(2223)	0.583(3)	0.284(2)	0.250(1)	27(1)
H(1)	0.32(1)	0.279(7)	0.153(5)	14(4)*

[a] The starred value indicates that the atom was refined isotropically. Anisotropically refined atoms are given in the form of the isotropic equivalent temperature factor defined as $(4/3)[a^2\beta(1,1) + b^2\beta(2,2) + c^2\beta(3,3) + ab(\cos\gamma)\beta(1,2) + ac(\cos\beta)\beta(1,3) + bc(\cos\alpha)\beta(2,3)]$.

observed at 275 nm (ϵ = 90 000 M^{-1} cm^{-1}). Ultraviolet irradiation ($\lambda > 290$ nm) of a benzene solution of **2** under an atmosphere of carbon dioxide led to the rapid decolorization of the solution. Ultraviolet photolysis in the absence of carbon dioxide led to identical results. Significantly, no reaction was observed to occur upon visible irradiation (λ = 550 nm) of the solution. The product isolated from the dark orange solution obtained subsequent to UV photolysis was characterized by conventional methods as well as by X-ray crystallography as the Arbuzov-type rearrangement product $[Ru_2H(CO)_5\{\mu\text{-}(Pr^iO)_2PN(Et)P(OPr^i)_2\}\{\mu\text{-}(Pr^iO)P(O)N(Et)P(OPr^i)_2\}]$ (**4**) (eq 1). The formation of **4** is accompanied by liberation of propene, as confirmed by gas chromatography. The $^{31}P\{^1H\}$ NMR spectrum of this compound exhibits a typical ABCX pattern with the ABC multiplet centered at δ 153 ppm and the X multiplet centered at δ 74.7 ppm. The ^1H NMR spectrum consists of an approximate quintet at δ -7.12 ppm, readily assigned to the hydride ligand. The IR spectrum

Table III. Selected Bond Lengths (Å) for Complex **4**[a]

Ru(1)-Ru(2)	2.894(1)	O(22)-C(22)	1.11(1)
Ru(1)-P(11)	2.357(3)	N(1B)-C(1B1)	1.49(1)
Ru(1)-P(12)	2.326(3)	N(2B)-C(2B1)	1.50(2)
Ru(1)-C(11)	1.91(2)	O(111)-C(1112)	1.45(1)
Ru(1)-C(12)	1.95(2)	O(121)-C(1212)	1.43(1)
Ru(1)-C(13)	1.90(2)	O(122)-C(1222)	1.43(2)
Ru(2)-P(21)	2.309(3)	O(211)-C(2112)	1.45(1)
Ru(2)-P(22)	2.306(4)	O(212)-C(2122)	1.44(2)
Ru(2)-C(21)	1.85(2)	O(221)-C(2212)	1.34(2)
Ru(2)-C(22)	1.95(2)	O(222)-C(2222)	1.30(3)
Ru(2)-H(1)	1.6(1)	C(1B1)-C(1B2)	1.49(2)
P(11)-O(111)	1.634(8)	C(2B1)-C(2B2)	1.43(3)
P(11)-O(112)	1.481(8)	C(1111)-C(1112)	1.51(2)
P(11)-N(1B)	1.72(1)	C(1112)-C(1113)	1.48(2)
P(12)-O(121)	1.601(9)	C(1211)-C(1212)	1.46(2)
P(12)-O(122)	1.57(1)	C(1212)-C(1213)	1.44(2)
P(12)-N(2B)	1.655(9)	C(1221)-C(1222)	1.49(2)
P(21)-O(211)	1.608(8)	C(1222)-C(1223)	1.46(2)
P(21)-O(212)	1.619(8)	C(2111)-C(2112)	1.49(2)
P(21)-N(1B)	1.643(9)	C(2112)-C(2113)	1.49(2)
P(22)-O(221)	1.52(1)	C(2121)-C(2122)	1.46(2)
P(22)-O(222)	1.61(1)	C(2122)-C(2123)	1.51(2)
P(22)-N(2B)	1.67(1)	C(2211)-C(2212)	1.40(4)
O(11)-C(11)	1.13(1)	C(2212)-C(2213)	1.34(5)
O(12)-C(12)	1.10(1)	C(2221)-C(2222)	1.54(3)
O(13)-C(13)	1.16(1)	C(2222)-C(2223)	1.25(3)
O(21)-C(21)	1.16(1)		

[a] Numbers in parentheses are estimated standard deviations in the least significant digits.

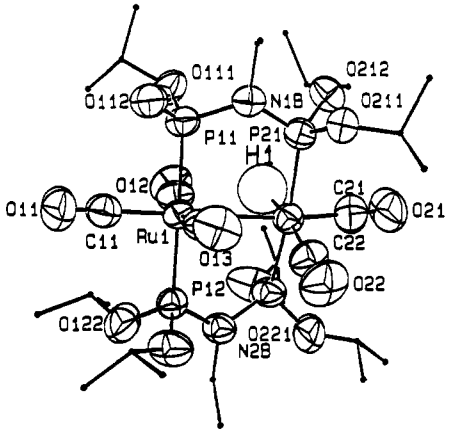

Figure 1. ORTEP drawing of $[Ru_2H(CO)_5\{\mu\text{-}(Pr^iO)_2PN(Et)P(OPr^i)_2\}\{\mu\text{-}(Pr^iO)P(O)N(Et)P(OPr^i)_2\}]$ (**4**).

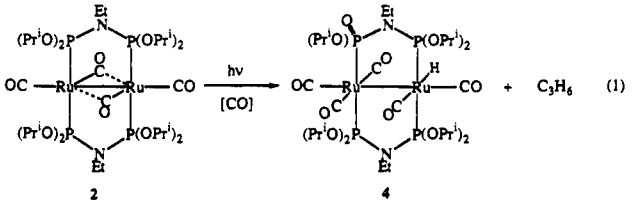

exhibits a set of peaks in the ν(CO) region [ν(C-O) 2057 w, 2019 s, 1985 s, 1963 sh, 1886 w cm^{-1} (THF)] in a band pattern typical of pentacarbonyl species of the type $[Ru_2L(CO)_5\{\mu\text{-}(RO)_2PN(Et)P(OR)_2\}_2]$.

The molecular structure of complex **4** is illustrated in Figure 1. The two ruthenium atoms are separated by a distance of 2.894(1) Å, corresponding to a ruthenium–ruthenium bond. The two ruthenium atoms are bridged both by a normal tetraisopropoxydiphosphazane ligand and by a $(Pr^iO)P(O)N(Et)P(OPr^i)_2$ phosphonate group, which clearly confirms the photochemically induced loss of an isopropyl radical from one of the diphosphazane ligands. The hydride ligand was located crystallographically and refined; it lies in an equatorial site, Ru(2)–H(1) = 1.6(1) Å, *trans* to one of the five CO ligands. Interestingly, the hydride is coordinated to a different ruthenium atom compared to the phosphorus atom of the $(Pr^iO)P(O)$ phosphonate fragment.

Table IV. Selected Bond Angles (deg) for Complex **4**

Ru(2)-Ru(1)-P(11)	92.66(9)	Ru(2)-P(22)-O(221)	120.3(5)
Ru(2)-Ru(1)-P(12)	88.82(9)	Ru(2)-P(22)-O(222)	118.2(4)
Ru(2)-Ru(1)-C(11)	179.5(4)	Ru(2)-P(22)-N(2B)	117.5(4)
Ru(2)-Ru(1)-C(12)	80.6(4)	O(221)-P(22)-O(222)	97.3(8)
Ru(2)-Ru(1)-C(13)	83.9(4)	O(221)-P(22)-N(2B)	100.7(6)
P(11)-Ru(1)-P(12)	178.0(1)	O(222)-P(22)-N(2B)	98.5(6)
P(11)-Ru(1)-C(11)	86.9(4)	P(11)-N(1B)-P(21)	124.0(6)
P(11)-Ru(1)-C(12)	89.8(4)	P(11)-N(1B)-C(1B1)	115.8(8)
P(11)-Ru(1)-C(13)	84.0(4)	P(12)-N(2B)-P(22)	120.1(6)
P(12)-Ru(1)-C(11)	91.6(4)	P(12)-N(2B)-C(2B1)	120.6(9)
P(12)-Ru(1)-C(12)	91.8(4)	P(22)-N(2B)-C(2B1)	118.5(8)
P(12)-Ru(1)-C(13)	94.8(4)	Ru(1)-C(11)-O(11)	179(2)
C(11)-Ru(1)-C(12)	99.1(6)	Ru(1)-C(12)-O(12)	176(1)
C(11)-Ru(1)-C(13)	96.4(6)	Ru(1)-C(13)-O(13)	175(1)
C(12)-Ru(1)-C(13)	163.0(6)	Ru(2)-C(21)-O(21)	178(1)
Ru(1)-Ru(2)-P(21)	88.48(9)	Ru(2)-C(22)-O(22)	176(1)
Ru(1)-Ru(2)-P(22)	88.3(1)	P(11)-O(111)-C(1112)	120.0(8)
Ru(1)-Ru(2)-C(21)	168.8(5)	P(12)-O(121)-C(1212)	125.7(9)
Ru(1)-Ru(2)-C(22)	91.9(4)	P(12)-O(122)-C(1222)	128(1)
Ru(1)-Ru(2)-H(1)	79(5)	P(21)-O(211)-C(2112)	122.9(7)
P(21)-Ru(2)-P(22)	171.2(1)	P(21)-O(212)-C(2122)	123.9(8)
P(21)-Ru(2)-C(21)	89.9(4)	P(22)-O(221)-C(2212)	135(1)
P(21)-Ru(2)-C(22)	95.9(4)	P(22)-O(222)-C(2222)	130(2)
P(21)-Ru(2)-H(1)	86(5)	N(1B)-C(1B1)-C(1B2)	113(1)
P(22)-Ru(2)-C(21)	91.8(4)	N(2B)-C(2B1)-C(2B2)	115(2)
P(22)-Ru(2)-C(22)	92.4(4)	O(111)-C(1112)-C(1111)	106(1)
P(22)-Ru(2)-H(1)	86(5)	O(111)-C(1112)-C(1113)	109(1)
C(21)-Ru(2)-C(22)	99.3(7)	C(1111)-C(1112)-C(1113)	110(2)
C(21)-Ru(2)-H(1)	90(5)	O(121)-C(1212)-C(1211)	113(1)
C(22)-Ru(2)-H(1)	171(4)	O(121)-C(1212)-C(1213)	105(1)
Ru(1)-P(11)-O(111)	111.2(3)	C(1211)-C(1212)-C(1213)	111(2)
Ru(1)-P(11)-O(112)	116.4(4)	O(122)-C(1222)-C(1221)	106(2)
Ru(1)-P(11)-N(1B)	111.1(3)	O(122)-C(1222)-C(1223)	109(2)
O(111)-P(11)-O(112)	109.3(5)	C(1221)-C(1222)-C(1223)	110(2)
O(111)-P(11)-N(1B)	99.9(5)	O(211)-C(2112)-C(2111)	109(1)
O(112)-P(11)-N(1B)	107.7(5)	O(211)-C(2112)-C(2113)	107(1)
Ru(1)-P(12)-O(121)	118.0(4)	C(2111)-C(2112)-C(2113)	111(1)
Ru(1)-P(12)-O(122)	199.3(4)	O(212)-C(2122)-C(2121)	107(1)
Ru(1)-P(12)-N(2B)	118.2(4)	O(212)-C(2122)-C(2123)	107(2)
O(121)-P(12)-O(122)	96.0(6)	C(2121)-C(2122)-C(2123)	111(1)
O(121)-P(12)-N(2B)	97.7(5)	O(221)-C(2212)-C(2211)	113(3)
O(122)-P(12)-N(2B)	103.5(5)	O(221)-C(2212)-C(2213)	113(4)
Ru(2)-P(21)-O(211)	117.1(3)	O(221)-C(2212)-C(2213)	113(4)
Ru(2)-P(21)-O(212)	114.7(3)	C(2211)-C(2212)-C(2213)	99(3)
Ru(2)-P(21)-N(1B)	119.7(4)	O(222)-C(2222)-C(2221)	103(2)
O(211)-P(21)-O(212)	97.6(5)	O(222)-C(2222)-C(2223)	130(4)
O(211)-P(21)-N(1B)	98.0(5)	C(2221)-C(2222)-C(2223)	103(2)
O(212)-P(21)-N(1B)	106.5(5)		

[a] Numbers in parentheses are estimated standard deviations in the least significant digits.

Furthermore the hydride is *trans* with respect to the ruthenium–ruthenium vector to the latter group. The compound adopts a partially staggered conformation as reflected by the P(11)–Ru(1)–Ru(2)–P(21) torsion angle of 9.93(12)°.

A proposed mechanism for the formation of **4** is presented in Scheme I. In the electronically unsaturated complex **2**, photolabilization of an isopropyl radical from the bridging isopropoxydiphosphazane ligand appears to occur more efficiently than photolabilization of CO. We note that complex **2** very efficiently scavenges CO to form **1**; and the fact that no traces of **1** can be observed during or after photolysis of **2** argues against CO loss as a primary photoprocess. Photolabilization of an isopropyl radical is followed by the β-elimination of propene and the formation of a hydride complex. An additional carbonyl ligand is however scavenged from some partial decomposition. Significantly, although the final product is a pentacarbonyl species, UV ($\lambda > 290$ nm) irradiation of the corresponding pentacarbonyl starting material, $[Ru_2(\mu\text{-CO})(CO)_4\{\mu\text{-}(Pr^iO)_2PN(Et)P(OPr^i)_2\}_2]$ (**1**), did not lead to any net photochemistry, indicating that the presence of a vacant site in **2** may be a necessary condition for the Arbuzov-type rearrangement to take place.

In the absence of β-hydrogen atoms, it is expected that the above reaction would terminate in the formation of alkyl migration products. Precedence for this reaction has been established by Pomeroy et al. Thermolysis of $[Ru\{P(OMe)_3\}_5]$ resulted in the formation of the Arbuzov-type product $[RuMe\{P(O)(OMe)_2\}\{P(OMe)_3\}_4]$, clearly illustrating the migration of a methyl group from a trimethyl phosphite ligand to the ruthenium metal center.[6] In order to better understand the photochemical Arbuzov reaction of **2**, photolysis of the tetramethoxydiphosphazane-bridged derivative $[Ru_2(\mu_{sb}\text{-CO})_2(CO)_2\{\mu\text{-}(MeO)_2PN(Et)P(OMe)_2\}_2]$ (**5**) was investigated in the hope of isolating the methyl migration product. Photolysis of **5** in benzene resulted in a yellow-orange solution from which no hydride chemical shift was detectable by ^1H NMR spectroscopy. The product was characterized by IR spectroscopy as well as by a partial X-ray diffraction study as the corresponding pentacarbonyl product $[Ru_2(\mu\text{-CO})(CO)_4\{\mu\text{-}(MeO)_2PN(Et)P(OMe)_2\}_2]$. In this case, the pentacarbonyl is the apparent result of a rapid scavenging of CO from decomposition products. Our results suggest that the final products obtained by the photolysis of electronically unsaturated complexes of the type $[Ru_2(\mu_{sb}\text{-CO})_2(CO)_2\{\mu\text{-}(RO)_2PN(Et)P(OR)_2\}_2]$ (R = Me, Pr^i) depend on a delicate balance between alkoxydiphosphazane ligand dealkylation and competing CO loss kinetic pathways. Transient absorption kinetic studies are planned on these and related compounds in order to determine in greater detail the nature and efficiencies of the primary photoprocesses responsible for this unprecedented Arbuzov-type photochemistry.

Scheme I

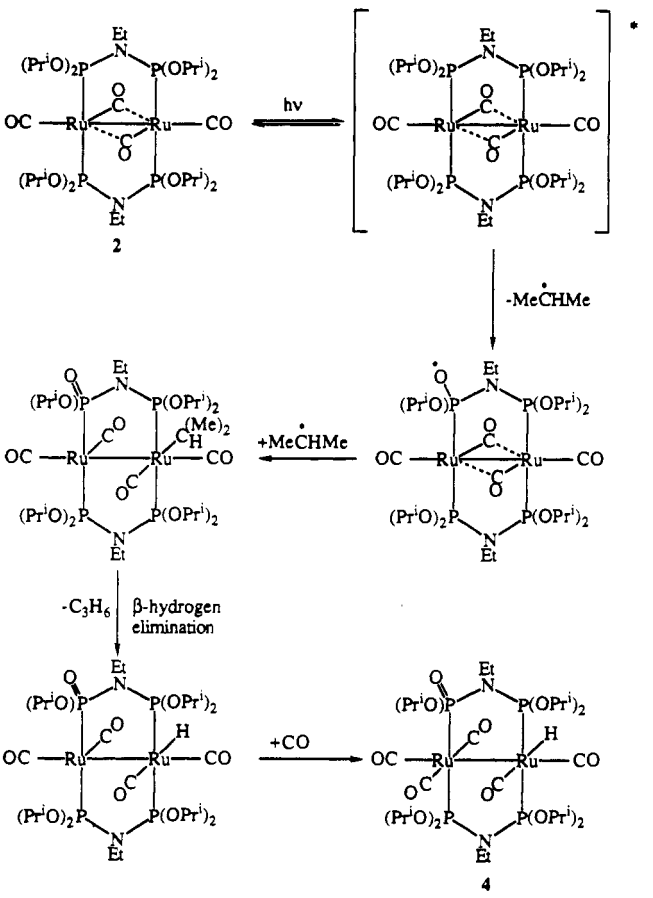

Acknowledgment. This research was supported by NSF Grant CHE-9016513 as well as by the Foundation for Research Development, South Africa. We are also grateful to the NSF for support of the Chemical X-ray Diffraction and Laser Facilities at Purdue and Dr. Steve Woolam for providing samples of $[Ru_2(\mu_{sb}\text{-CO})_2(CO)_2\{\mu\text{-}(RO)_2PN(Et)P(OR)_2\}_2]$ (R = Me, Pr^i). R.M.G. gratefully acknowledges a NASA Graduate Fellowship.

Supplementary Material Available: For **4**, a general description of experimental procedures in the collection and refinement of X-ray data and tables of crystal and data collection parameters, positional parameters and their estimated standard deviations for hydrogen atoms, general temperature factors, β_{ij}, bond distances, bond angles, and torsional angles (22 pages). Ordering information is given on any current masthead page.